

## ARTICLE OPEN



# m6A RNA methylation-mediated NDUFA4 promotes cell proliferation and metabolism in gastric cancer

Weihong Xu<sup>1,2</sup>, Yanan Lai<sup>2</sup>, Yunqi Pan<sup>2</sup>, Meiyu Tan<sup>2</sup>, Yanyun Ma<sup>3</sup>, Huiming Sheng<sup>2</sup> and Jiucun Wang<sup>1</sup>

© The Author(s) 2022

Gastric cancer (GC) is a malignancy with poor prognosis. NDUFA4 is reported to correlate with the progression of GC. However, its underlying mechanism in GC is unknown. Our study was to reveal the pathogenic mechanism of NDUFA4 in GC. NDUFA4 expression was explored in single-cell and bulk RNA-seq data as well as GC tissue microarray. Mitochondrial respiration and glycolysis were estimated by oxygen consumption rate and extracellular acidification rate, respectively. The interaction between NDUFA4 and METTL3 was validated by RNA immunoprecipitation. Flow cytometry was used to estimate cell cycle, apoptosis and mitochondrial activities. NDUFA4 was highly expressed in GC and its high expression indicated a poor prognosis. The knockdown of NDUFA4 could reduce cell proliferation and inhibit tumor growth. Meanwhile, NDUFA4 could promote glycolytic and oxidative metabolism in GC cells, whereas the inhibition of glycolysis suppressed the proliferation and tumor growth of GC. Besides, NDUFA4 inhibited ROS level and promoted MMP level in GC cells, whereas the inhibition of mitochondrial fission could reverse NDUFA4-induced glycolytic and oxidative metabolism and tumor growth of GC. Additionally, METTL3 could increase the m6A level of NDUFA4 mRNA via the m6A reader IGF2BP1 to promote NDUFA4 expression in GC cells. Our study revealed that NDUFA4 was increased by m6A methylation and could promote GC development via enhancing cell glycolysis and mitochondrial fission. NDUFA4 was a potential target for GC treatment.

*Cell Death and Disease* (2022)13:715; <https://doi.org/10.1038/s41419-022-05132-w>

## INTRODUCTION

Gastric cancer (GC) is a malignancy ranked as the fourth occurrence of cancer [1]. Every year, more than 1 million GC cases are diagnosed and it causes hundreds of thousands of deaths. Current management of GC is composed of surgery, chemotherapy, radiotherapy, and immunotherapy. However, despite the great progress of cancer treatment, the 5-year survival of GC patients is <30% [2]. Therefore, it is urgent to have a better understanding of GC development.

Cancer is heterogeneous and various cancers use both glycolysis and oxidative phosphorylation for energy metabolism. The cell survival, proliferation, invasion, metastasis, and drug resistance of GC are energy-demanding processes, fuelled by glycolysis and oxidative metabolism [3]. Shift metabolism profile from mitochondrial oxidative phosphorylation to aerobic glycolysis is a key for tumor cell growth and metastasis [4]. As such, dysfunctional changes in cellular energy metabolism in GC warrant further investigation.

NADH dehydrogenase (ubiquinone) 1 alpha subcomplex 4 (NDUFA4), which encodes a subunit of the electron transport chain complex belonging to the respiratory chain of mitochondria to produce ATP [5]. Since tumor cells tend to evade apoptosis, the regulation of mitochondria-mediated cell death is commonly detected in different tumors [6]. This resistance of apoptosis is associated with mitochondrial dynamics, including fusion and fission, which are reported to closely correlate with cancer development [7].

NDUFA4 is reported to be differentially expressed in renal cell carcinoma and is associated with cancer-specific survival [8]. NDUFA4 could contribute to the growth and metastasis of human lung cancer cells through altering the transduction of the AKT and ERK pathways [9]. NDUFA4 promotes proliferation, reduces apoptosis and activates the oxidative phosphorylation pathway of GC cells [10]. Moreover, NDUFA4 facilitates glycolysis rather than oxidative phosphorylation in colorectal cancer cells by regulating genes involved in glycolysis [11].

N6-methyladenosine (m6A) methylation is involved in the initiation and development of cancers [12]. The m6A process is regulated by three types of protein, including methyltransferases ("writers"), binding proteins ("readers"), and demethylases ("erasers"). METTL3 is one of the writers and it often works with IGF2BP1, a reader protein, during m6A methylation [13–15]. The role of m6A regulators has been widely depicted in different cancers such as glioma [16], esophageal cancer [17], colorectal cancer [18], and GC [19], etc. However, its role in regulating NDUFA4 expression is unclear.

A previous study indicated that long non-coding RNA (lncRNA) MIF-AS1 could increase NDUFA4 expression to promote GC progression [10]. However, the mechanism of NDUFA4 in GC required additional investigation. Herein, our study was to comprehensively explore the pathogenic mechanism of NDUFA4 in GC.

<sup>1</sup>School of Life Sciences, Fudan University, Shanghai 200433, China. <sup>2</sup>Department of Clinical Laboratory, Shanghai Tongren Hospital, Shanghai 200336, China. <sup>3</sup>Department of Anthropology and Human Genetics, School of Life Sciences, Fudan University, Shanghai 200438, China. <sup>✉</sup>email: xwh3066@126.com; jcwang@fudan.edu.cn  
Edited by Professor Anastasis Stephanou

Received: 30 March 2022 Revised: 22 July 2022 Accepted: 25 July 2022

Published online: 17 August 2022

## MATERIALS AND METHODS

### Bioinformatics analysis

The RNA expression data of GC were acquired from Gene Expression Omnibus (GEO) database, in which single-cell RNA-seq data were obtained from GSE134520 dataset [20] and bulk RNA-seq data were obtained from GSE33335 dataset [21]. The prognostic value of NDUFA4 in GC patients was analyzed using the GEO database provided by the Kaplan–Meier plotter (kmplot.com/analysis).

### Clinical specimens

The 30 paired GC and adjacent-normal specimens were collected from patients who received surgery at Shanghai Tongren Hospital from July 2019 to July 2021. This study was approved by the Ethics Committee of the Shanghai Tongren Hospital with written informed consent obtained. Besides, the GC tissue microarray that included 95 GC tissues and 20 normal gastric tissues was purchased from Shanghai Outdo Biotech. The inclusion criteria was defined as the certain diagnosis of GC. Also, patients who had received any treatment such as chemotherapy, radiotherapy, and biological medication (monoclonal antibodies) before the sampling were excluded from the study.

### Immunohistochemistry (IHC)

The clinical specimens in paraffin were sectioned. The anti-NDUFA4 antibody (bs-19070R; BLOSS) was applied to the section followed by the secondary antibody (D-3004, Shanghai Long Island Biotech. Co., Ltd). The expression of NDUFA4 was scored by two investigators blinded to clinical status, based on staining intensity (0, negative; 1, weak; 2, moderate; 3, strong) and percentage of positive cells (0, <5%; 1, 5–25%; 2, 25–50%; 3, 50–75%; 4, >75%). GC patients were divided into low- and high-expression groups based on the cutoff point of IHC score = 6.

### Cell culture and transfection

The human GC cell lines (AGS, HGC27, MKN28, MKN45, and MGC-803) and normal human gastric epithelium (GES-1) were obtained from Shanghai Cell Bank and authenticated by STR before shipping. Mycoplasma contamination was tested if concerned. Cells were cultured in DMEM with 10% fetal bovine serum (Gibco, Grand Island, NY, USA). siRNAs targeting METTL3 were synthesized by GenePharma. The shRNAs targeting NDUFA4 or IGF2BP1 were cloned into a pLKO.1 vector and packaged as lentivirus. The sequences of shRNA and siRNAs were listed in Supplementary Table 1.

### Cell viability

Cells were seeded in 96-well plates ( $3 \times 10^3$ /well) and incubated with 10  $\mu$ l Cell Counting Kit-8 reagent for 1 h. Then the optical density at 450 nm was detected.

### Colony formation assay

Forty-eight hours after treatment, cells were seeded in 10 cm dishes and cultured for two weeks. At the end of the incubation, colonies were fixed with paraformaldehyde for 15 min and stained with 0.5% crystal violet for 30 min. Colonies with 50 cells or more were counted.

### Flow cytometry

Cells were fixed using 70% ethanol and stained by propidium iodide (PI) for cell cycle analysis. PI and FITC-labeled annexin V (annexin V–FITC) staining were used for cell apoptosis analysis. Besides, 10  $\mu$ M 2'-7'-dichlorofluorescein diacetate (DCFH-DA) was used to estimate reactive oxygen species (ROS) level. Moreover, mitochondrial membrane potential (MMP) ratio was calculated as red (JC-1 aggregates)/green (JC-1 monomers) fluorescence intensity using JC-1 assay kit (C2006, Beyotime Institute of Biotechnology, Jiangsu, China). Flow cytometry was conducted on CytoFLEX flow cytometry (BD Biosciences, Franklin Lakes, NJ, USA).

### Extracellular flux analysis

The level of oxygen consumption rate (OCR) and extracellular acidification rate (ECAR) was estimated using Seahorse XF24 Extracellular Flux Analyzer as previously described [22]. Briefly, cells digested to a density of  $1 \times 10^4$ /well, were seeded in XF-24 culture plates (Agilent Technologies, Santa Clara, CA, USA), and were then placed in an incubator of 37 °C and 5% CO<sub>2</sub> for 24 h. Around 1 h before detection, cells were shifted into an incubator without CO<sub>2</sub>, and culture medium was replaced by XF Base Medium

(Agilent Technologies). Subsequently, 1  $\mu$ M oligomycin (ATP synthase inhibitor) was added into “A” well of Seahorse gauging plate, 1.5  $\mu$ M carbonyl cyanide p-trifluoromethoxyphenylhydrazone (FCCP; uncoupler) was supplemented into “B” well and then mixture of antimycin A (complex III inhibitor; 0.5  $\mu$ M) & rotenone (complex I inhibitor; 0.5  $\mu$ M) was instilled into “C” well using Seahorse XF Cell Mito Stress Test Kit (Agilent Technologies). Using a Seahorse XF24 Extracellular Flux Analyzer, cellular OCR was monitored. In addition, the cells were treated sequentially with 1  $\mu$ M of glucose, 1  $\mu$ M of oligomycin, and 0.5  $\mu$ M of 2-DG (the glycolytic inhibitor) at time points for measurement of ECAR.

### Measurement of glucose uptake

Glucose uptake was measured using a fluorescent glucose 2-NBDG (2-Deoxy-2-[(7-nitro-2,1,3-benzoxadiazol-4-yl) Glucose Uptake Assay Kit (Biovision, Milpitas, CA, USA) following manufacturer’s protocol. In brief,  $5 \times 10^5$  cells per well in a six-well plate were cultured at 37 °C for 24 h. At 48 h after transduction, cells were starved for glucose for 3 h. After incubating with Krebs-Ringer Bicarbonate Buffer with 2% bovine serum albumin for 40 min, 2-NBDG (100  $\mu$ M) was injected into each well and incubated for 45 min at 37 °C. The cells were then washed with PBS, trypsinized, resuspended in 10% FBS before subjecting to flow cytometry analysis. The glucose uptake potential of the samples was analyzed using CytoFLEX flow cytometer (BD Biosciences).

### Measurement of lactate and ATP

The cells were seeded in 96-well plates at  $3.5 \times 10^3$  cells per well. After overnight incubation at 37 °C, 5% CO<sub>2</sub>, the complete medium was changed to fresh DMEM (50  $\mu$ l/well). After 24 h, the supernatant of cells was collected by centrifugation. Then, according to the manufacturer’s instructions, the lactate release was determined using Lactic Acid assay kit (Nanjing Jiancheng Bioengineering Institute, China). ATP content was measured with the ATP assay kit (Nanjing Jiancheng Bioengineering Institute, China), as per the manufacturer’s protocol. In brief, cells were seeded in the 6-well plate for 12–24 h. Then cells were harvested by using 200–300  $\mu$ l lysis buffer and vortexed for 1 min. The supernatant was mixed with detection solution and then analysis for ATP concentration was normalized to the corresponding total protein amounts from each sample.

### Quantitative RT-PCR (qRT-PCR)

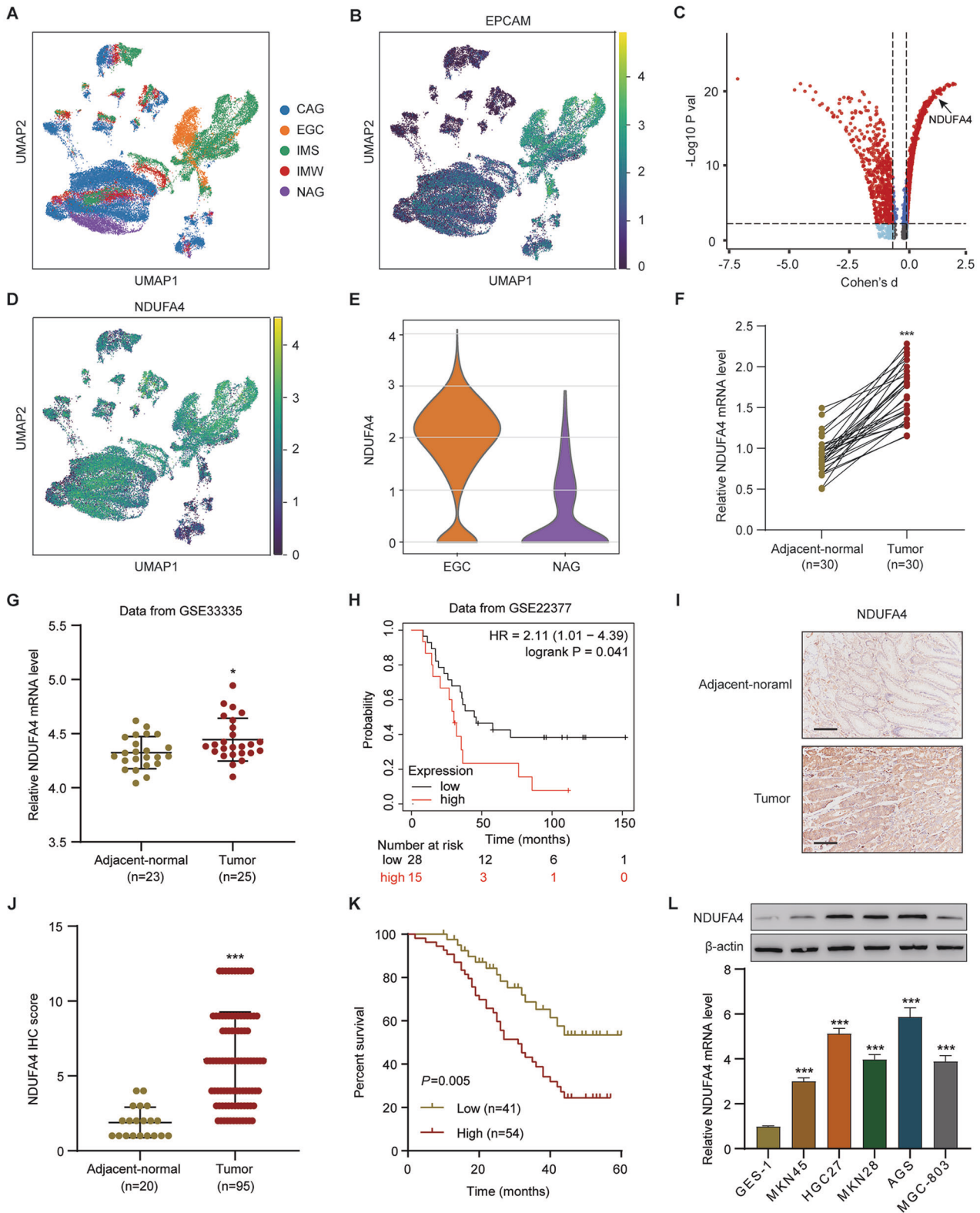
Total RNA was extracted using Trizol reagents. The qRT-PCR was performed using SYBR® Green kit on QuantStudio 5 system (ABI, USA). Gene expression was normalized to  $\beta$ -actin. The primer sequences were listed as follows: NDUFA4-F: 5'-AGTCCGTAGTGTCTCATTG-3', NDUFA4-R: 5'-TACAGTGTGCTCCAGTAG-3'; Cyclin D1-F: 5'-AGTCTGTGCTCGAAGTGG AAC-3', Cyclin D1-R: 5'-AGTGTCAATGAAATCGTGGGGGT-3'; CDK4-F: 5'-GCCTGGCCAGAATCTACAGCTAC-3', CDK4-R: 5'-GGTCCGGCTTCAGAGTTTCCA C-3';  $\beta$ -actin-F: 5'-TGGCATCCACGAACTAC-3',  $\beta$ -actin-R: 5'-CTTGATCTTCAT GGTGCTG-3'.

### Western blot

The total protein was extracted by RIPA buffer, separated by SDS-PAGE, and transferred to PVDF membrane. Then it was blocked and incubated with antibodies against NDUFA4 (ab129752), OPA1 (ab157457), p-Drp1 (ab154879), PGC1 $\alpha$  (ab106814), ENO1 (ab227978), LDHA (ab101562), METTL3 (ab195352), IGF2BP1 (ab184305), Cyclin D1 (ab16663), CDK4 (ab108357) and  $\beta$ -actin (ab8226, all from Abcam). The protein content was detected by enhanced chemiluminescence system (Bio-Rad, USA).

### Analysis of m<sup>6</sup>A content

Trizol reagent was used to extract the total RNA. Poly(A)<sup>+</sup> RNA was purified using GenElute™ mRNA Miniprep Kit (MRN10, Sigma, Louis, MO, USA). The m<sup>6</sup>A content was assayed using the m<sup>6</sup>A RNA Methylation Assay Kit (ab185912, Abcam). Briefly, 80  $\mu$ l of binding solution and 200 ng of sample RNA were added into each designated well, and then incubated at 37 °C for 90 min for RNA binding. Wash each well three times with wash buffer. 50  $\mu$ l of the diluted capture antibody was added into each well, and then incubated at room temperature for 60 min. Each well was incubated with detection antibody and enhancer solution at room temperature for 30 min subsequently. Finally, the wells were incubated with developer solution in the dark for 1 to 10 min at 25 °C. The reaction was stopped with stop solution and determined using a microplate reader at 450 nm wavelength within 2 to 10 min.



### RNA immunoprecipitation (RIP) assays

Magna RIP RNA-Binding Protein Immunoprecipitation kit (Millipore Sigma, Burlington, MA, USA) was used for the RIP assay following the manufacturer's instructions. Cells were prepared using RIP lysis buffer and the RNA-protein complexes were incubated with anti-m6A (ab208577), anti-IGF2BP1 (ab184305) or anti-IgG antibody (ab172730, all from Abcam) overnight at 4°C and washed with RIP-wash buffer for 10 min at 4°C and then RIP-lysis

buffer for 5 min at 4°C. The co-precipitated RNAs were purified using phenol:chloroform:isoamyl alcohol and subjected to qRT-PCR.

### Dual-luciferase reporter assay

The NDUFA4 3'UTR sequence was cloned into the pG3 vector (Promega, Madison, WI, USA). GC cells were transfected with METTL3 siRNA and the

**Fig. 1** **NDUFA4 was up-regulated in GC and its elevation indicated poor prognosis.** **A** Uniform Manifold Approximation and Projection (UMAP) plot of patients with non-atrophic gastritis (NAG), chronic atrophic gastritis (CAG), wild intestinal metaplasia (IMW), severe intestinal metaplasia (IMS) and EGC in GSE134520 are denoted by distinct colors. **B** UMAP plot showed the distribution of epithelial cells in patients with NAG, CAG, IMW, IMS and EGC, marked by the expression of marker gene epithelial cell adhesion molecule (EPCAM) (yellow, high; purple, low). **C** Differentially expressed genes in epithelial cells between patients with EGC and NAG (the significantly expressed gene, NDUFA4, is highlighted). **D** UMAP plot of NDUFA4 expression in patients with NAG, CAG, IMW, IMS and EGC (yellow, high; purple, low). **E** NDUFA4 expression in epithelial cells between patients with EGC and NAG. **F, G** NDUFA4 expression in paired gastric and adjacent normal tissues in hospital cohort (**F**) and GSE33335 dataset (**G**). **H** Survival analysis and comparison among people with high and low values of NDUFA4 expression in GSE22377 database. **I** Representative IHC images and (**J**) scores of NDUFA4 in GC tissue microarrays. Scale bar: 100  $\mu$ m. **K** Survival analysis and comparison among people with high and low expression of NDUFA4 expression in GC tissue microarrays. **L** The relative mRNA and protein levels of NDUFA4 in various GC cells and normal human gastric epithelium. \* $P < 0.05$ , \*\*\* $P < 0.001$  vs adjacent-normal or GES-1.

pGI3-NDUFA4 3'UTR luciferase reporter plasmid and the pRL-TK vector (Promega) expressing the Renilla luciferase) using Lipofectamine 2000 (Invitrogen). A dual-luciferase assay was conducted based on the manufacturer's protocol. The firefly luciferase activity was normalized to the Renilla luciferase activity.

#### Estimation of mRNA stability

Cells were treated with 0.2 mM actinomycin D (GlpBio, Montclair, CA, USA) for 0, 3, and 6 h. The samples were then collected for total RNA extraction and cDNA synthesis, which were performed according to the methods described above. qRT-PCR was performed for the quantification of mRNA levels.

#### In vivo tumor xenograft model

All animal experiments were performed under the animal ethics guidelines of Shanghai Tongren Hospital. A total of  $5 \times 10^7$  AGS cells transduced with or without NDUFA4 shRNA or MKN45 cells transduced with or without NDUFA4 overexpression lentivirus were subcutaneously injected into nude mice (4–6 weeks) ( $n = 6$  each group). The 2-DG (100 mg/kg/day) and mitochondrial fission inhibitor Mdivi-1 (25 mg/kg/day) were administered after 12 days of injection. Tumor size was detected every 3 days. The xenografts were collected after 33 days.

#### Statistical analysis

Data analyses and visualization were conducted using GraphPad Prism 8.4.2. For difference comparison, the data followed a normal distribution, as confirmed by Shapiro-Wilk test. Thus, the student t-test and one-way ANOVA were used. Kaplan-Meier was used for survival analysis.  $P < 0.05$  was statistically significant.

## RESULTS

### NDUFA4 was increased in GC and its elevation indicated unfavorable prognosis

The single-cell RNA-seq data of patients with gastric premalignant lesions and early gastric cancer (EGC) were downloaded from the GEO database with accession number [GSE134520](#). This data set consists of 56,440 cells from patients with non-atrophic gastritis (NAG), chronic atrophic gastritis (CAG), wild intestinal metaplasia (IMW), severe intestinal metaplasia (IMS) and EGC, which are structures by Uniform Manifold Approximation and Projection (UMAP) and denoted by distinct colors (Fig. 1A). UMAP plot showed the distribution of epithelial cells in patients with NAG, CAG, IMW, IMS and EGC, marked by the expression of marker gene epithelial cell adhesion molecule (EPCAM) (Fig. 1B). To determine whether the genes exert differential effects on GC tumorigenesis, we compared the single cell RNA-seq transcriptome of each epithelial cell between patients with EGC and NAG, and differentially expressed transcripts were shown in Fig. 1C, among which NDUFA4 expression in patients with NAG, CAG, IMW, IMS and EGC was also analyzed by UMAP (Fig. 1D). Moreover, NDUFA4 expression in epithelial cells from patients with EGC was higher than that with NAG (Fig. 1E). In our 30 paired GC and normal specimens, NDUFA4 was significantly elevated in GC specimens (Fig. 1F). Similarly, NDUFA4 had high expression in GC tissues than adjacent normal tissues in GSE33335 dataset (Fig. 1G). Moreover, the low expression NDUFA4 was associated with the favorable prognosis in GC patients in GSE22377 dataset (Fig. 1H). In

GC tissue microarray, the protein expression of NDUFA4 was also elevated in GC specimens, and its high expression indicated poor prognosis (Fig. 1I–K). Furthermore, the expression of NDUFA4 was notably correlated with two of the clinicopathologic characteristics, tumor size and TNM stage, in the patients with GC (Supplementary Table 2). Compared with human normal gastric epithelium, the expression of NDUFA4 were significantly elevated in GC cells especially in AGS and HGC27 (Fig. 1L). Therefore, NDUFA4 was highly expressed in GC and indicated poor prognosis in GC patients.

### NDUFA4 promoted cell proliferation and cell cycle and reduced apoptosis in GC cells

Then we explored the functions of NDUFA4 in GC cells. Since NDUFA4 had high expression in AGS and HGC27, and its expression was relatively low in MKN45 cells, we transduced NDUFA4 shRNA in AGS and HGC27 cells (Supplementary Fig. 1A), and overexpression lentivirus in MKN45 cells (Supplementary Fig. 1A). The knockdown of NDUFA4 significantly reduced the viability of AGS and HGC27 cells, whereas its overexpression significantly promoted the cell viability in MKN45 cells (Fig. 2A). Similarly, the colony formation was significantly inhibited by shNDUFA4 but promoted by overexpressed NDUFA4 (Fig. 2B, C). Flow cytometry revealed that the proportion of GC cells arrested at G0-G1 phase was significantly promoted by the knockdown of NDUFA4 and inhibited by overexpressed NDUFA4 (Fig. 2D, E). Western blot analysis showed that the expression of Cyclin D1 and CDK4 was inhibited by knockdown of NDUFA4 and promoted by overexpressed NDUFA4 (Supplementary Fig. 1B). Pearson correlation analysis also demonstrated the positive correlation between NDUFA4 and Cyclin D1 or CDK4 in patients with GC in the hospital cohort (Supplementary Fig. 1C, D). Moreover, cell apoptosis was significantly promoted by the knockdown of NDUFA4 in AGS and HGC27 cells and inhibited by overexpressed NDUFA4 in MKN45 cells (Supplementary Fig. 2A–C). These findings suggested that NDUFA4 could promote proliferation and cell cycle and inhibit apoptosis in GC cells.

### NDUFA4 promoted GC growth in vivo

Further, we verified the oncogenic role of NDUFA4 in mice. AGS cells transduced with shNDUFA4 or shNC and MKN45 cells transduced with NDUFA4 overexpression vector or blank vector were subcutaneously injected in mice. After the sacrifice of mice, we found that the tumor volume and tumor weight in shNDUFA4 group was significantly lower than shNC group (Fig. 3A, B). Western blot analysis showed that the expression of Cyclin D1 and CDK4 in tumor xenograft was inhibited by knockdown of NDUFA4 (Fig. 3C). In contrast, the overexpression of NDUFA4 significantly promoted tumor growth and expression of Cyclin D1 and CDK4 in tumor xenograft (Fig. 3D–F). These results demonstrated that NDUFA4 could promote tumor growth in GC mice model.

### NDUFA4 promotes glycolytic and oxidative metabolism in GC cells

Given that cell survival, proliferation and function are an energy-demanding process [23], we subsequently explored the potential

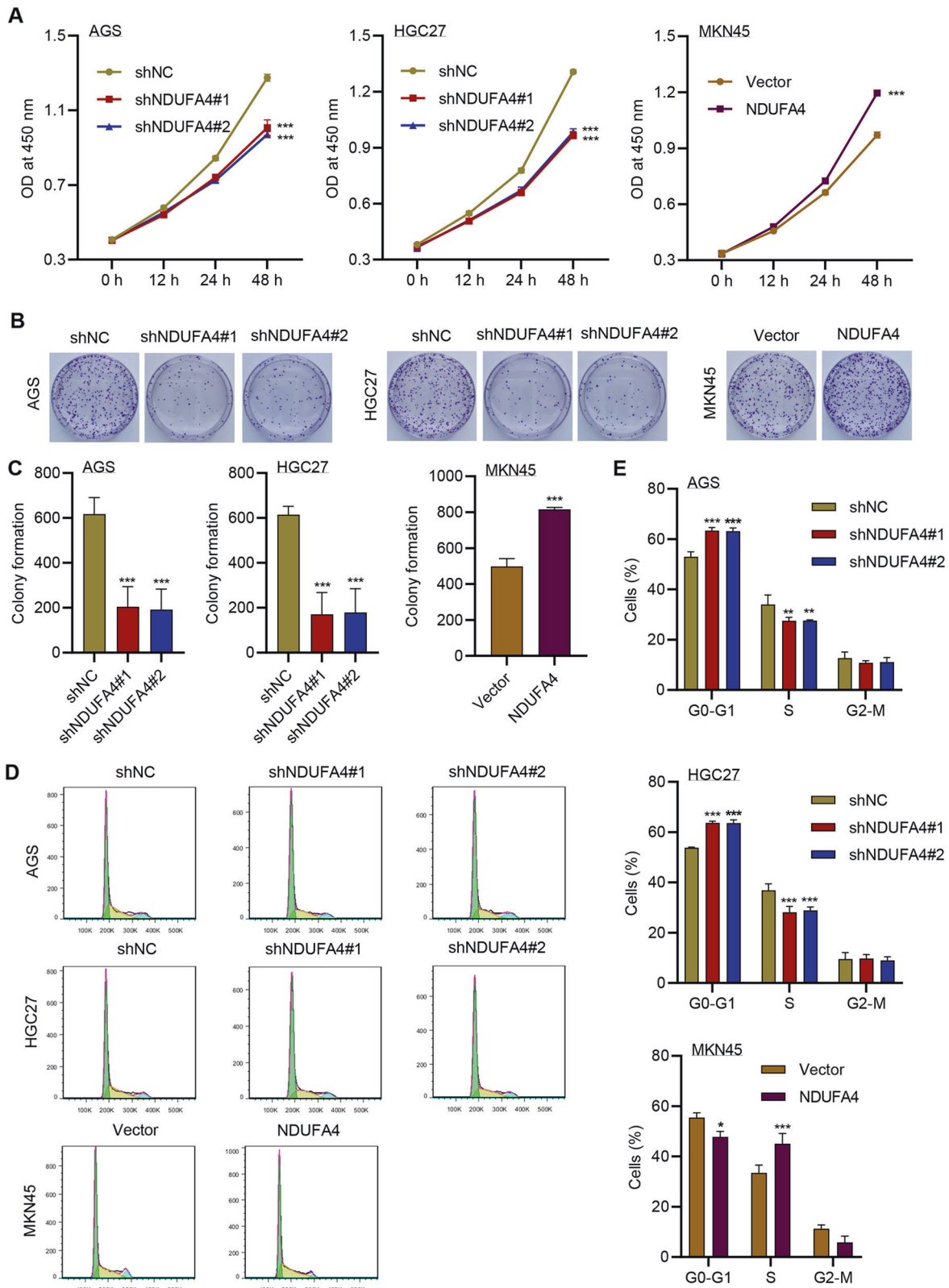


**Fig. 2** NDUFA4 promoted cell proliferation and reduced cell cycle arrest and apoptosis in GC cells. **A** Cell viability, **(B, C)** colony formation and **(D, E)** cell cycle of AGS, HGC27 and MKN45 cells with or without NDUFA4 overexpression or knockdown. \* $P < 0.05$ , \*\* $P < 0.01$ , \*\*\* $P < 0.001$  vs shNC or vector.

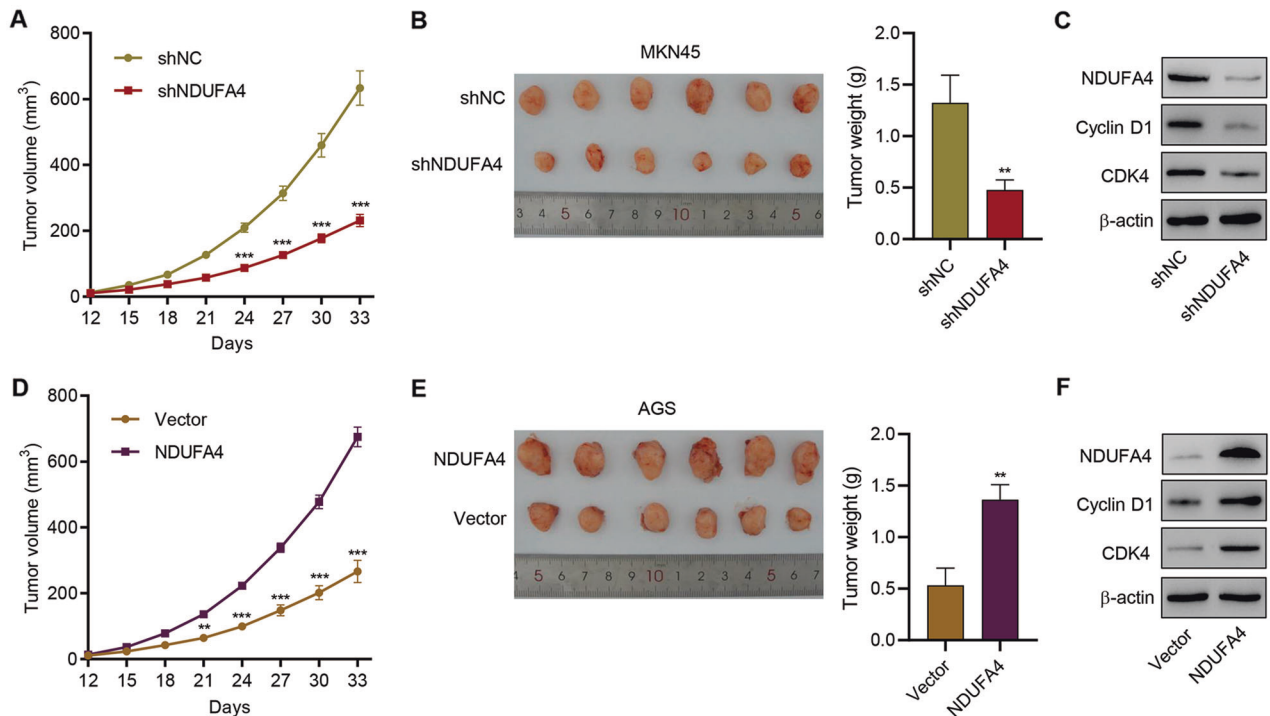


**Fig. 3 NDUF4A promoted GC growth in vivo.** AGS cells transduced with shNC or NDUF4A shRNA vector and MKN45 cells transduced with NDUF4A expression vector were subcutaneously injected into the armpits of the nude mice, respectively. **A, D** Tumor volume in each group. **B, E** Tumor weight in each group. **C, F** Expression of NDUF4A, Cyclin D1 and CDK4 in each group. \*\*\* $P < 0.001$  vs. shNC or vector.

effects of NDUF4A on glycolytic and oxidative metabolism in GC cells. Glucose uptake was significantly inhibited by the knockdown of NDUF4A in AGS and HGC27 cells and promoted by over-expressed NDUF4A in MKN45 cells (Supplementary Fig. 3A, B). The knockdown of NDUF4A significantly diminished the ECAR and OCR of AGS and HGC27 cells whereas the elevation of NDUF4A significantly promoted ECAR and OCR in MKN45 cells (Fig. 4A, B, Supplementary Fig 4A, B). Moreover, the level of lactate and ATP was significantly reduced by the knockdown of NDUF4A and promoted by the overexpression of NDUF4A (Fig. 4C, D). Western blot analysis showed that the expression of glycolytic enzymes ENO1 and LDHA was significantly inhibited by the knockdown of NDUF4A and promoted by overexpressed NDUF4A (Fig. 4E). These findings indicated that NDUF4A could promote glycolytic and oxidative metabolism in GC cells.

#### Inhibition of glycolysis exerted anti-tumor effects against GC

Further, we employed glycolysis inhibitor, 2-DG, to explore the role of glycolysis in GC. The application of 10 mM 2-DG significantly inhibited the viability of AGS and MKN45 (Fig. 5A). The colony formation was also significantly suppressed by 2-DG (Fig. 5B). Moreover, the proportion of G0-G1 phase cells was significantly promoted by 2-DG (Fig. 5C, D). In mice, the administration of 2-DG significantly reduced the tumor growth in mice (Fig. 5E–G). These results demonstrated that the suppression of glycolysis could inhibit the proliferation and progression of GC.

#### NDUF4A regulated the level of ROS and MMP in GC cells

We also explored the correlation between NDUF4A and mitochondrial activities in GC cells. The ROS level was significantly elevated by the knockdown of NDUF4A in AGS cells, whereas the promotion of NDUF4A significantly reduced the ROS level in MKN45 cells (Fig. 6A, B). Besides, the knockdown of NDUF4A significantly reduced the MMP and the overexpression of NDUF4A exerted opposite effects (Fig. 6C, D). Meanwhile, OPA1,

phosphorylated-Drp1 (p-Drp1) and PGC1 $\alpha$  were reported to correlate with mitochondrial fusion, fission and biogenesis [24–26]. Western blot revealed that the shNDUF4A markedly reduced the expression of OPA1, p-Drp1, and PGC1 $\alpha$  whereas its overexpression exerted opposite effects (Fig. 6E). Therefore, these results indicated that NDUF4A could regulate mitochondrial dynamics and biogenesis in GC cells.

#### Inhibition of mitochondrial fission reversed NDUF4A-mediated effects in GC

Then we applied mitochondrial fission inhibitor, Mdivi-1, to verify the correlation between NDUF4A and mitochondrial fission in GC. The application of 20  $\mu$ M Mdivi-1 significantly reduced the viability of MKN45 cells, which was opposite to NDUF4A-mediated effects (Fig. 7A). Besides, the level of glucose uptake, ECAR and OCR was significantly promoted by NDUF4A and reversed by Mdivi-1 (Fig. 7B, C, Supplementary Fig. 5A–C). Meanwhile, the production of lactate and ATP was significantly elevated by NDUF4A but reversed by Mdivi-1 (Fig. 7D, E). In GC-bearing mice, the application of Mdivi-1 significantly reduced the tumor growth in NDUF4A and vector groups (Fig. 7F–H). Therefore, the inhibition of mitochondrial fission could exert opposite effects against NDUF4A in GC.

#### METTL3 promoted the m6A methylation of NDUF4A via the m6A reader IGF2BP1

Then we investigated the upstream regulation of NDUF4A in GC cells. m6A modification sites of NDUF4A were predicted by SRAMP. To further examine whether NDUF4A expression is modulated by RNA methylation, AGS cells were treated with 3-Deazaadenosine (DAA), an inhibitor of RNA methylation. The application of 100  $\mu$ M DAA significantly reduced the expression of NDUF4A in AGS cells (Fig. 8A), which indicated the potential regulatory role of mRNA methylation in NDUF4A expression. The inhibition of METTL3 could reduce the whole m6A level of AGS cells as well as that of the 3'UTR region of NDUF4A mRNA (Fig. 8B,

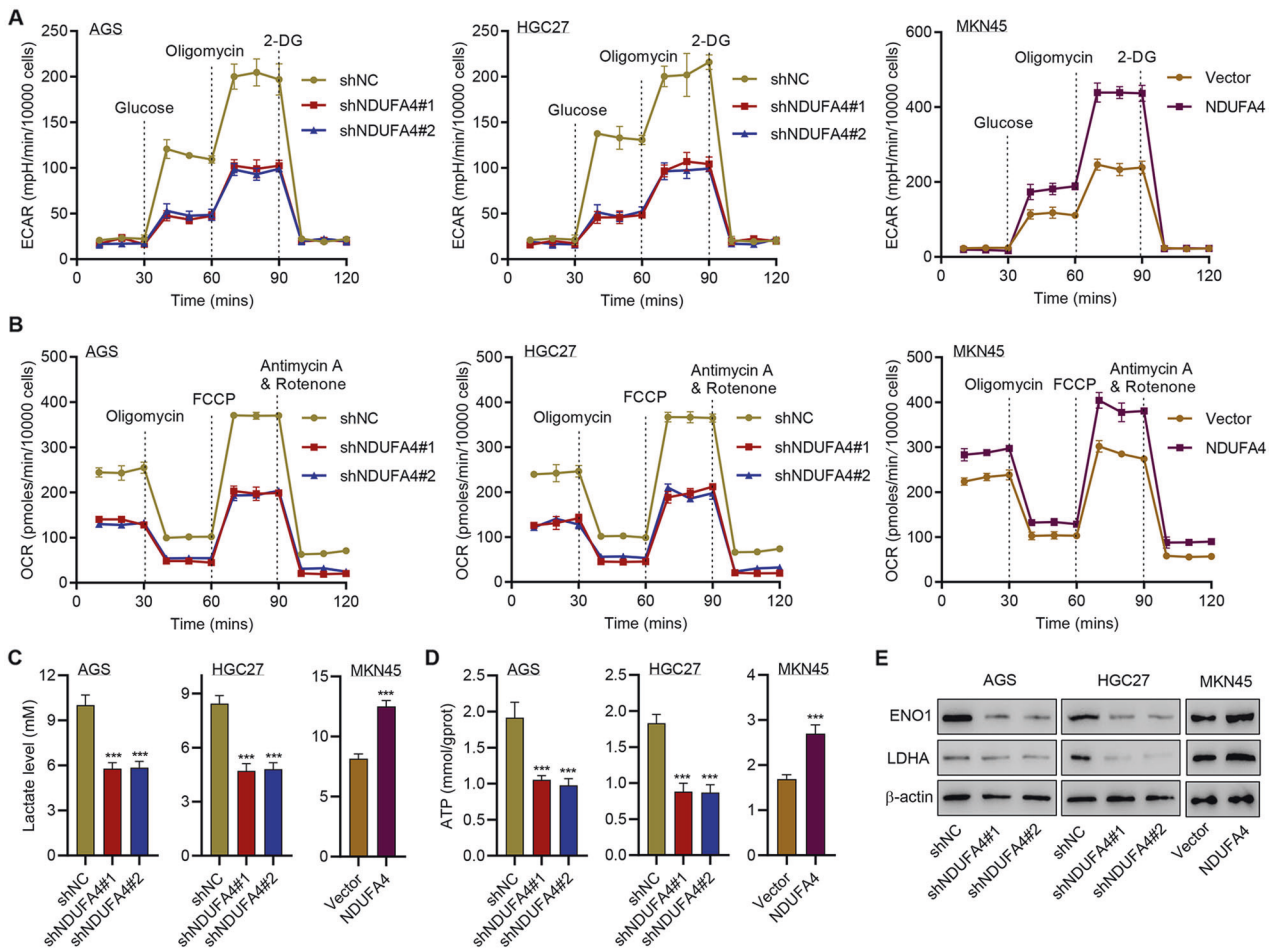


**Fig. 4** **NDUFA4 promotes glycolytic and oxidative metabolism in GC cells.** **A** ECAR, **(B)** OCR, **(C)** lactate, **(D)** ATP content and **(E)** expression of ENO1 and LDHA in AGS, HGC27 and MKN45 cells with or without NDUFA4 overexpression or knockdown. \*\*\* $P < 0.001$  vs shNC or vector.

C). Moreover, the knockdown of METTL3 significantly reduced the luciferase activity of NDUFA4 mRNA (Fig. 8D). Also, it also reduced the expression of METTL3 and NDUFA4 (Fig. 8E, F). Meanwhile, we found that the transduction of shRNAs targeting IGF2BP1 could significantly reduce the expression of IGF2BP1, which led to the reduction of NDUFA4 mRNA stability (Fig. 8G, H). RIP assay demonstrated that IGF2BP1 could bind with the 3'UTR region of NDUFA4 mRNA (Fig. 8I). These results suggested that METTL3 could increase the m6A level of NDUFA4 mRNA via the m6A reader IGF2BP1 to promote the expression of NDUFA4.

## DISCUSSION

The pathogenic mechanism underlying GC development remains to be clarified. Our study revealed that NDUFA4 was highly expressed in GC and its high expression indicated a poor prognosis. The knockdown of NDUFA4 could reduce cell proliferation and inhibit tumor growth. Meanwhile, NDUFA4 could promote glycolytic and oxidative metabolism in GC cells, whereas the inhibition of glycolysis suppressed the proliferation and tumor growth of GC. Besides, NDUFA4 inhibited ROS level and promoted MMP level in GC cells, whereas the inhibition of mitochondrial fission could reverse NDUFA4-induced glycolytic and oxidative metabolism and tumor growth of GC. Additionally, METTL3 could increase m6A level of NDUFA4 mRNA via the m6A reader IGF2BP1 to promote NDUFA4 expression in GC cells (Supplementary Fig. 6). Therefore, our study uncovered a novel pathogenic mechanism of GC progression and provided a potential target for GC treatment.

NDUFA4 is reported to correlate with the development of lung cancer [9], clear cell renal cell carcinoma [8], and colorectal cancer [11]. NDUFA4 was a biomarker for cancer-specific survival of patients with clear cell renal cell carcinoma [8]. Besides, NDUFA4 was the target of miR-7 that promoted the progression of lung cancer cells via activating AKT and ERK pathways [9]. Moreover, NDUFA4 was involved in the oncogenic mechanism of lncRNA MIFG-AS1 in colorectal cancer [11]. In GC, NDUFA4 was upregulated by lncRNA MIF-AS1, which could promote proliferation and reduce cell apoptosis [10]. This result was consistent with our findings that NDUFA4 was highly expressed in GC and correlated with the poor prognosis of GC patients. Gastric adenocarcinoma is histologically divided into intestinal, diffuse, mixed, and indeterminate subtypes, whereas the diffuse type of GC usually has a shorter duration of disease and poor prognosis [27]. Our results have revealed that NDUFA4 was highly expressed in all HER2-negative GC cell lines compared with normal human gastric epithelium, in which intestinal-type GC cell lines (MKN28, AGS) showed higher NDUFA4 expression in comparison to intestinal diffuse-type GC cell lines (MKN45). Therefore, further study is needed to fully elucidate the role and expression pattern of NDUFA4 in different histological forms of GC. In GC, NDUFA4 could promote cell proliferation and tumor growth. Therefore, NDUFA4 was implicated to play an oncogenic role in GC and was a potential target for GC treatment.

Cell metabolisms such as glycolysis and mitochondrial dynamics, including fusion and fission were distinct characteristics of cancer cells [28, 29]. Several studies have shown that NDUFA4

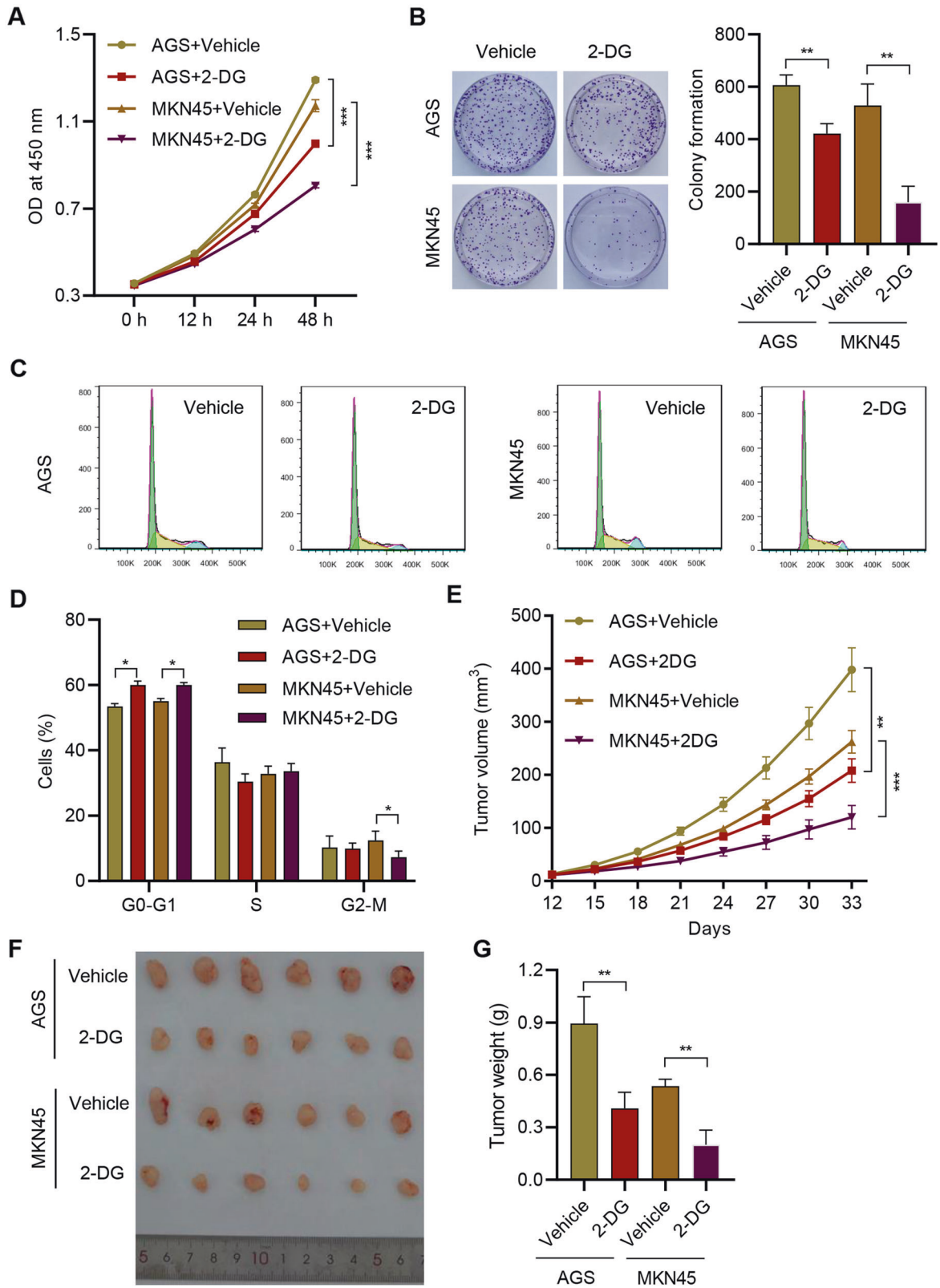


**Fig. 5** Inhibition of glycolysis exerted anti-tumor effects against GC. **A** Cell viability, **(B)** colony formation and **(C, D)** cell cycle of AGS and MKN45 cells treated with 10 mM 2-DG or vehicle. AGS or MKN45 cells were subcutaneously injected into the mice with or without 100 mg/kg 2-DG treatment. **E** Tumor volume was estimated. **F** The photograph of tumors. **G** Tumor weight in each group. \*\* $P < 0.01$ , \*\*\* $P < 0.001$ .



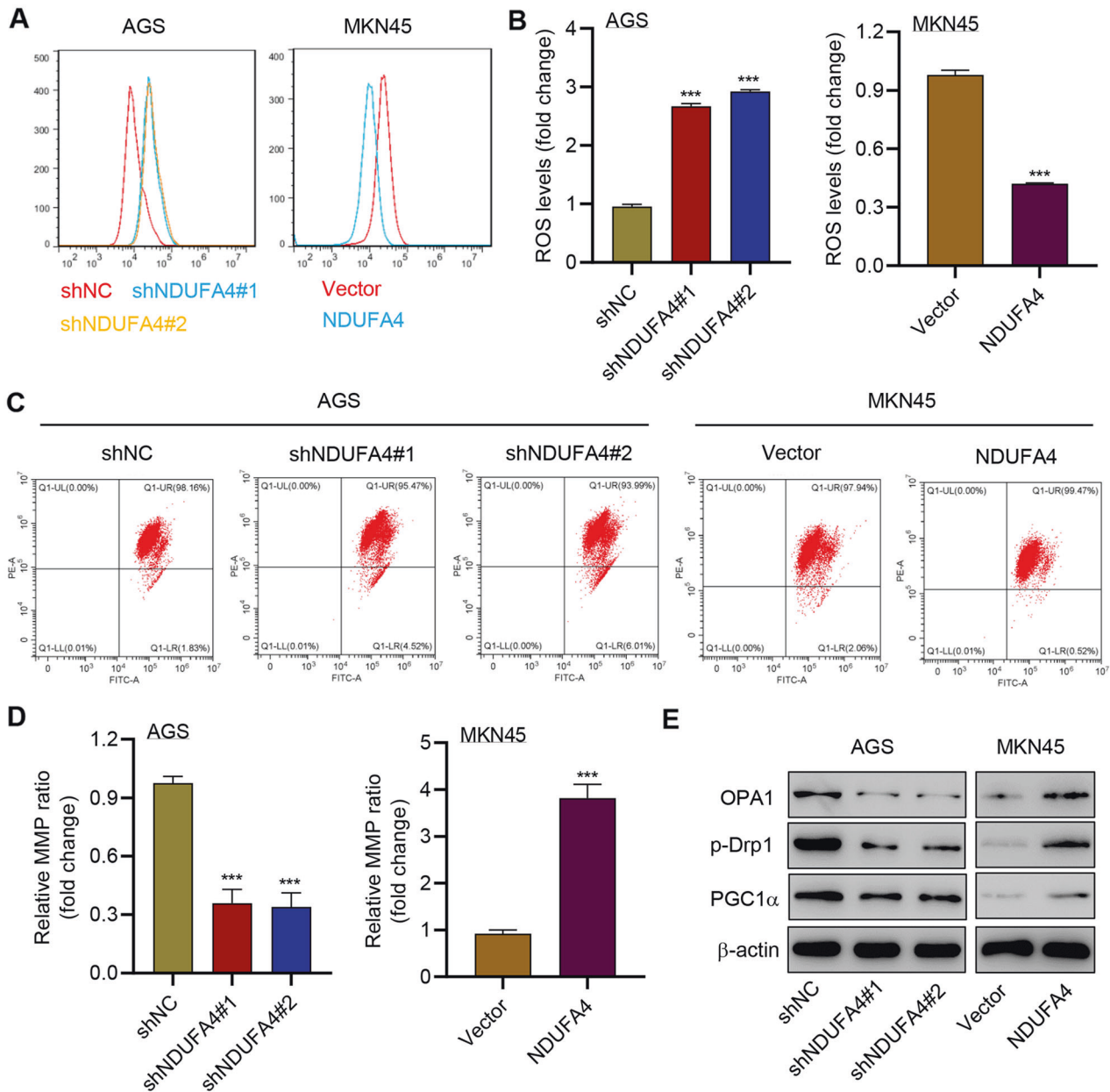


**Fig. 6** NDUFA4 regulated the level of ROS and MMP in GC cells. (A, B) ROS, (C, D) MMP and (E) expression of OPA1, p-Drp1 and PGC1 $\alpha$  in AGS and MKN45 cells modulated as indicated. \*\*\* $P < 0.001$  vs shNC or vector.

encodes a subunit of the electron transport chain complex belonging to the respiratory chain of mitochondria to produce ATP, regulates oxidative phosphorylation pathway-related proteins such as COX6C, COX5B and NDUFA8 in GC cells [10], and promotes glucose uptake, lactate production and major enzymes involved in glycolysis such as PDK1, PFK1, PKM2 in colorectal cancer cells [11]. We demonstrated that NDUFA4 promotes glycolysis by regulating the expression of glycolytic enzymes, including ENO1 and LDHA and modulates mitochondrial dynamics and biogenesis by regulating the expression of OPA1, p-Drp1, and PGC1 $\alpha$ . Previous studies have reported that NDUFA4 promotes the progression of lung cancer cells via activating PI3K/AKT pathway [9] and the PI3K/AKT pathway is responsible for glycolysis by regulating HIF-1 $\alpha$  target genes ENO1 and LDHA [30, 31]. These data indicate that NDUFA4 may regulate ENO1 and LDHA expression via the PI3K/AKT/HIF-1 $\alpha$  signaling pathway. However, whether other glycolytic enzymes are regulated by

NDUFA4 should be further determined. It is possible that NDUFA4 facilitates glycolytic/oxidative metabolism by regulating these proteins. The elevation of cell glycolysis was demonstrated to promote cancer progression [32]. In addition, not only cell viability and proliferation, but also tumor metastasis and metabolism were accelerated by glycolysis and mitochondrial dynamics and biogenesis [33–37]. The lactate produced by glycolysis increased cell motility and drug resistance and its expression in tumors strongly indicated metastasis [38, 39]. In this study, we found that NDUFA4 could promote cell glycolysis and lactate production in GC, whereas the inhibition of glycolysis by 2-DG could reverse NDUFA4-mediated effects on tumor growth in vitro and in vivo. Since ROS level and MMP were essential for mitochondrial fission and they were significantly mediated by NDUFA4. Moreover, the inhibition of mitochondrial fission by Mdivi-1 could reverse NDUFA4-mediated effects on glycolytic/oxidative metabolism in vitro and tumor growth in vivo. Therefore, our results revealed

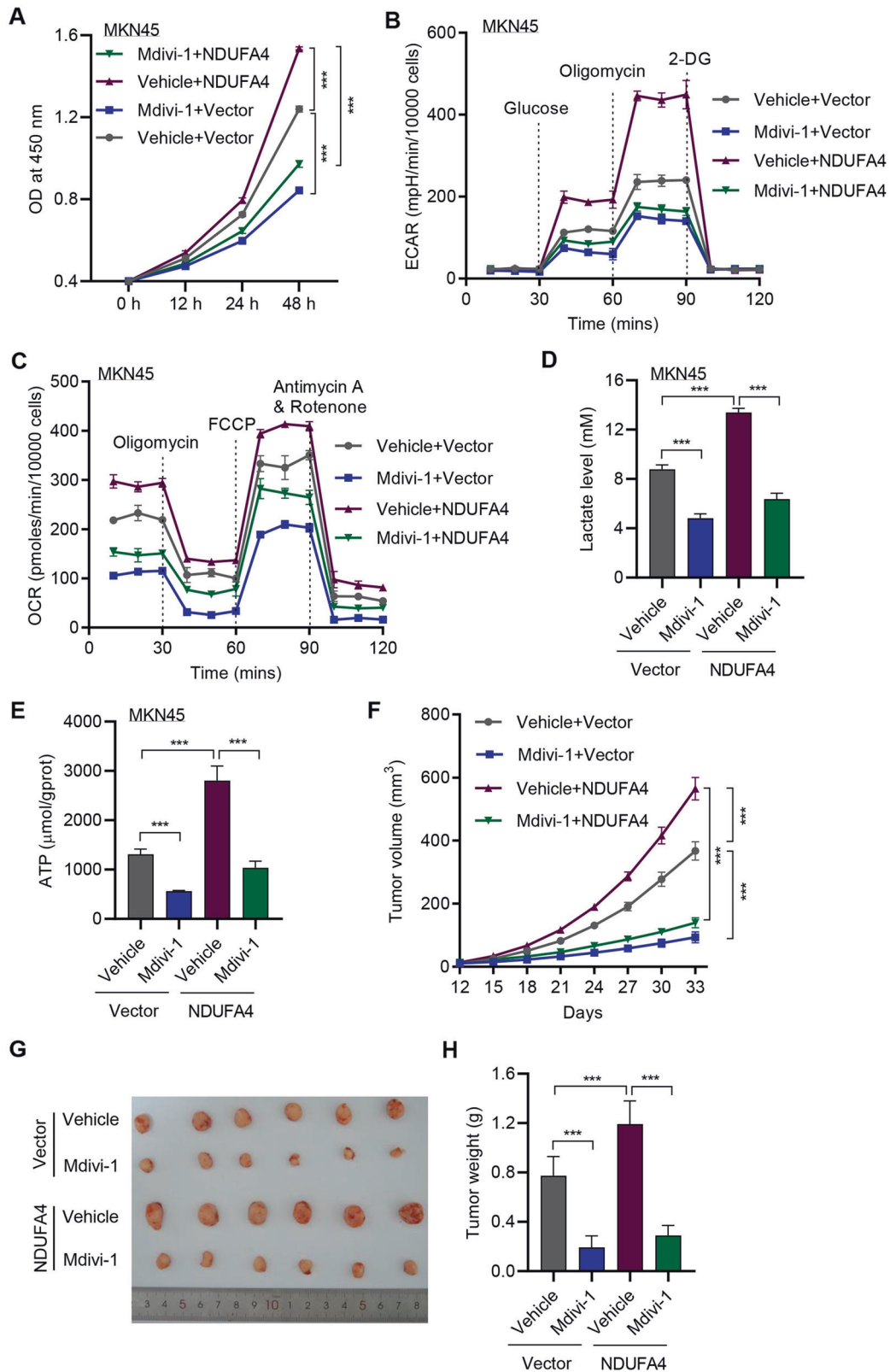


**Fig. 7** Inhibition of mitochondrial fission reversed NDUFA4-mediated effects in GC. **A** Cell viability, **(B)** ECAR, **(C)** OCR, **(D)** lactate and **(E)** ATP content of MKN45 cells with NDUFA4 overexpression and/or 20  $\mu\text{M}$  Mdivi-1. MKN45 cells transduced with NDUFA4 expression vector were subcutaneously injected into the armpits of the mice with or without 25 mg/kg Mdivi-1 treatment. **F** Tumor volume in each group. **G** The photograph of xenografts. **H** Tumor weight in each group.  $***P < 0.001$ .

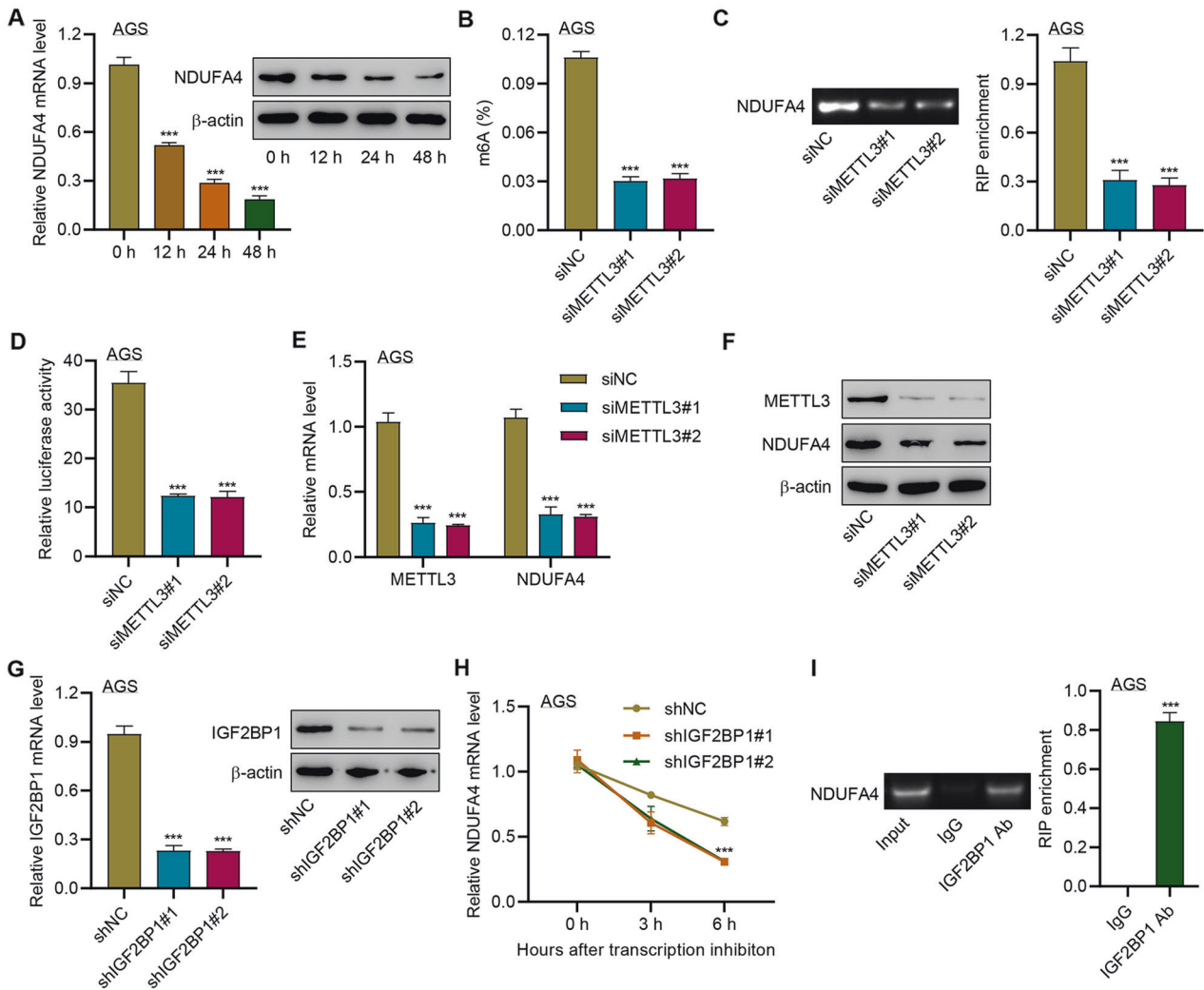


**Fig. 8** METTL3 promoted the m6A modification of NDUFA4 via the m6A reader IGF2BP1. **A** NDUFA4 expression in AGS cells treated with 100  $\mu$ M 3-Deazaadenosine (DAA) for 0, 12, 24, and 48 h. **B–F** AGS cells were transfected with METTL3 siRNA. The whole m6A level (**B**), m6A level of NDUFA4 3'UTR (**C**), and abundance of NDUFA4 3'UTR (**D**) were detected. The expression of METTL3 (**E**) and NDUFA4 (**F**) was detected. **G–H** IGF2BP1 expression (**G**) and NDUFA4 mRNA stability (**H**) in AGS cells transfected with IGF2BP1 shRNA. **I** The interaction between IGF2BP1 and NDUFA4 3'UTR was detected by RIP assay. \*\*\* $P < 0.001$  vs 0 h, siNC, shNC or IgG.

that the GC progression might benefit from glycolytic/oxidative metabolism. Nevertheless, further study is need to fully validate the correlation between glycolytic/oxidative metabolism and GC progression.

METTL3 is one of the m6A writers and is involved in the development of various cancers [40]. Wang et al. revealed that the overexpression of METTL3 in GC cells resulted in the significantly promoted m6A level [41]. Besides, METTL3 was shown to promote the methylation of SEC62 mRNA that was stabilized by IGF2BP1, and the increased expression of SEC62 could promote the proliferation of GC cells [42]. However, the association between METTL3 and NDUFA4 in GC remained unclear. Herein, our study revealed that NDUFA4 expression was significantly reduced by DAA, a potent inhibitor of methyltransferase activity. METTL3 could promote the m6A level of NDUFA4 mRNA via the reader IGF2BP1. Our study revealed the upstream regulation of NDUFA4 that contributed to the progression of GC. Previous studies showed that the expression of m6A writers (METTL3, RBM15, WTAP), eraser (FTO, ALKBH5) and reader (YTHDF3, YTHDC2) was associated with pathological stage, tumor stage, and prognosis of patients with GC [43, 44]. IGF2BP2 and IGF2BP3 also regulated GC cell proliferation, migration and

invasion [45, 46]. Therefore, whether other writers, erasers and readers contribute to the m6A methylation of NDUFA4 in GC cells need to be further confirmed.

To sum up, our study revealed that NDUFA4 was increased by m6A methylation and could promote GC development via enhancing cell glycolysis and mitochondrial fission. NDUFA4 was a potential target for GC treatment.

#### DATA AVAILABILITY

All data presented in this study are included within the paper and its Supplementary files.

#### REFERENCES

- Torre LA, Bray F, Siegel RL, Ferlay J, Lortet-Tieulent J, Jemal A. Global cancer statistics, 2012. *CA Cancer J Clin*. 2015;65:87–108.
- Allemani C, Weir HK, Carreira H, Harewood R, Spika D, Wang XS, et al. Global surveillance of cancer survival 1995–2009: analysis of individual data for 25,676,887 patients from 279 population-based registries in 67 countries (CONCORD-2). *Lancet (Lond, Engl)*. 2015;385:977–1010.
- Liu W, Zhao ZM, Liu YL, Pan HF, Lin LZ. Weipiling ameliorates gastric precancerous lesions in *Atp4a(-/-)* mice. *BMC Complement Alter Med*. 2019;19:318.

4. Zhao X, Zhu Y, Hu J, Jiang L, Li L, Jia S, et al. Shikonin Inhibits Tumor Growth in Mice by Suppressing Pyruvate Kinase M2-mediated Aerobic Glycolysis. *Sci Rep*. 2018;8:14517.
5. Balsa E, Marco R, Perales-Clemente E, Szklarczyk R, Calvo E, Landazuri MO, et al. NDUFA4 is a subunit of complex IV of the mammalian electron transport chain. *Cell Metab*. 2012;16:378–86.
6. Fulda S. Tumor resistance to apoptosis. *Int J Cancer*. 2009;124:511–5.
7. Rodrigues T, Ferraz LS. Therapeutic potential of targeting mitochondrial dynamics in cancer. *Biochem Pharm*. 2020;182:114282.
8. Muller FE, Braun M, Syring I, Klumper N, Schmidt D, Perner S, et al. NDUFA4 expression in clear cell renal cell carcinoma is predictive for cancer-specific survival. *Am J Cancer Res*. 2015;5:2816–22.
9. Lei L, Chen C, Zhao J, Wang H, Guo M, Zhou Y, et al. Targeted Expression of miR-7 Operated by TTF-1 Promoter Inhibited the Growth of Human Lung Cancer through the NDUFA4 Pathway. *Mol Ther Nucleic Acids*. 2017;6:183–97.
10. Li L, Li Y, Huang Y, Ouyang Y, Zhu Y, Wang Y, et al. Long non-coding RNA MIF-AS1 promotes gastric cancer cell proliferation and reduces apoptosis to upregulate NDUFA4. *Cancer Sci*. 2018;109:3714–25.
11. Cui S, Yang X, Zhang L, Zhao Y, Yan W. LncRNA MAFG-AS1 promotes the progression of colorectal cancer by sponging miR-147b and activation of NDUFA4. *Biochem Biophys Res Commun*. 2018;506:251–8.
12. Yang Y, Hsu PJ, Chen YS, Yang YG. Dynamic transcriptomic m(6)A decoration: writers, erasers, readers and functions in RNA metabolism. *Cell Res*. 2018;28:616–24.
13. Meyer KD, Jaffrey SR. Rethinking m(6)A Readers, Writers, and Erasers. *Annu Rev Cell Dev Biol*. 2017;33:319–42.
14. Wang S, Sun C, Li J, Zhang E, Ma Z, Xu W, et al. Roles of RNA methylation by means of N(6)-methyladenosine (m(6)A) in human cancers. *Cancer Lett*. 2017;408:112–20.
15. Zaccara S, Ries RJ, Jaffrey SR. Reading, writing and erasing mRNA methylation. *Nat Rev Mol Cell Biol*. 2019;20:608–24.
16. Xu S, Tang L, Dai G, Luo C, Liu Z. Expression of m6A Regulators Correlated With Immune Microenvironment Predicts Therapeutic Efficacy and Prognosis in Gliomas. *Front Cell Dev Biol*. 2020;8:594112.
17. Xu LC, Pan JX, Pan HD. Construction and Validation of an m6A RNA Methylation Regulators-Based Prognostic Signature for Esophageal Cancer. *Cancer Manag Res*. 2020;12:5385–94.
18. Ji L, Chen S, Gu L, Zhang X. Exploration of Potential Roles of m6A Regulators in Colorectal Cancer Prognosis. *Front Oncol*. 2020;10:768.
19. Su Y, Huang J, Hu J. m(6)A RNA Methylation Regulators Contribute to Malignant Progression and Have Clinical Prognostic Impact in Gastric Cancer. *Front Oncol*. 2019;9:1038.
20. Zhang P, Yang M, Zhang Y, Xiao S, Lai X, Tan A, et al. Dissecting the Single-Cell Transcriptome Network Underlying Gastric Premalignant Lesions and Early Gastric Cancer. *Cell Rep*. 2019;27:1934–47.e5.
21. Cheng L, Yang S, Yang Y, Zhang W, Xiao H, Gao H, et al. Global gene expression and functional network analysis of gastric cancer identify extended pathway maps and GPRC5A as a potential biomarker. *Cancer Lett*. 2012;326:105–13.
22. Guo Y, Liang F, Zhao F, Zhao J. Resibufogenin suppresses tumor growth and Warburg effect through regulating miR-143-3p/HK2 axis in breast cancer. *Mol Cell Biochem*. 2020;466:103–15.
23. Tan J, Ni D, Ribeiro RV, Pinget GV, Macia L. How Changes in the Nutritional Landscape Shape Gut Immunometabolism. *Nutrients*. 2021;13.
24. Zhang Y, Wang Y, Xu J, Tian F, Hu S, Chen Y, et al. Melatonin attenuates myocardial ischemia-reperfusion injury via improving mitochondrial fusion/mitophagy and activating the AMPK-OPA1 signaling pathways. *J Pineal Res*. 2019;66:e12542.
25. Schmitt K, Grimm A, Dallmann R, Oettinghaus B, Restelli LM, Witzig M, et al. Circadian Control of DRP1 Activity Regulates Mitochondrial Dynamics and Bioenergetics. *Cell Metab*. 2018;27:657–66.e5.
26. Tian L, Cao W, Yue R, Yuan Y, Guo X, Qin D, et al. Pretreatment with Tiliarin improves mitochondrial energy metabolism and oxidative stress in rats with myocardial ischemia/reperfusion injury via AMPK/SIRT1/PGC-1 alpha signaling pathway. *J Pharm Sci*. 2019;139:352–60.
27. Pavlovic M, Gajovic N, Jurisevic M, Mitrovic S, Radosavljevic G, Pantic J, et al. Diverse Expression of IL-32 in Diffuse and Intestinal Types of Gastric Cancer. *Gastroenterol Res Pr*. 2018;2018:6578273.
28. Libertini MV, Locasale JW. The Warburg Effect: How Does it Benefit Cancer Cells? *Trends Biochem Sci*. 2016;41:211–8.
29. Srinivasan S, Guha M, Kashina A, Avadhani NG. Mitochondrial dysfunction and mitochondrial dynamics-The cancer connection. *Biochim Biophys Acta Bioenerg*. 2017;1858:602–14.
30. Pan T, Sun S, Chen Y, Tian R, Chen E, Tan R, et al. Immune effects of PI3K/Akt/HIF-1 $\alpha$ -regulated glycolysis in polymorphonuclear neutrophils during sepsis. *Crit Care*. 2022;26:29.
31. Reece KM, Richardson ED, Cook KM, Campbell TJ, Pisle ST, Holly AJ, et al. Epi-dithiodiketopiperazines (ETPs) exhibit in vitro antiangiogenic and in vivo anti-tumor activity by disrupting the HIF-1 $\alpha$ /p300 complex in a preclinical model of prostate cancer. *Mol Cancer*. 2014;13:91.
32. Lu CW, Lin SC, Chen KF, Lai YY, Tsai SJ. Induction of pyruvate dehydrogenase kinase-3 by hypoxia-inducible factor-1 promotes metabolic switch and drug resistance. *J Biol Chem*. 2008;283:28106–14.
33. Rehman J, Zhang HJ, Toth PT, Zhang Y, Marsboom G, Hong Z, et al. Inhibition of mitochondrial fission prevents cell cycle progression in lung cancer. *FASEB J*. 2012;26:2175–86.
34. Zhao J, Zhang J, Yu M, Xie Y, Huang Y, Wolff DW, et al. Mitochondrial dynamics regulates migration and invasion of breast cancer cells. *Oncogene*. 2013;32:4814–24.
35. Inoue-Yamauchi A, Oda H. Depletion of mitochondrial fission factor DRP1 causes increased apoptosis in human colon cancer cells. *Biochem Biophys Res Commun*. 2012;421:81–5.
36. Han T, Kang D, Ji D, Wang X, Zhan W, Fu M, et al. How does cancer cell metabolism affect tumor migration and invasion? *Cell Adh Migr*. 2013;7:395–403.
37. Zhang Z, Li TE, Chen M, Xu D, Zhu Y, Hu BY, et al. MFN1-dependent alteration of mitochondrial dynamics drives hepatocellular carcinoma metastasis by glucose metabolic reprogramming. *Br J Cancer*. 2020;122:209–20.
38. Fanciulli M, Bruno T, Giovannelli A, Gentile FP, Di Padova M, Rubio O, et al. Energy metabolism of human LoVo colon carcinoma cells: correlation to drug resistance and influence of Ionidamine. *Clin Cancer Res*. 2000;6:1590–7.
39. Hirschhaeuser F, Sattler UG, Mueller-Klieser W. Lactate: a metabolic key player in cancer. *Cancer Res*. 2011;71:6921–5.
40. Zeng C, Huang W, Li Y, Weng H. Roles of METTL3 in cancer: mechanisms and therapeutic targeting. *J Hematol Oncol*. 2020;13:117.
41. Wang Q, Chen C, Ding Q, Zhao Y, Wang Z, Chen J, et al. METTL3-mediated m(6)A modification of HDGF mRNA promotes gastric cancer progression and has prognostic significance. *Gut*. 2020;69:1193–205.
42. He H, Wu W, Sun Z, Chai L. MiR-4429 prevented gastric cancer progression through targeting METTL3 to inhibit m(6)A-caused stabilization of SEC62. *Biochem Biophys Res Commun*. 2019;517:581–7.
43. Zhang C, Zhang W, Ge S, Huang W, Lin X, Gao J, et al. Reduced m6A modification predicts malignant phenotypes and augmented Wnt/PI3K-Akt signaling in gastric cancer. *Cancer Med*. 2019;8:4766–81.
44. Jing JJ, Zhao X, Li H, Sun LP, Yuan Y. Expression profiles and prognostic roles of m6A writers, erasers and readers in gastric cancer. *Future Oncol*. 2021;17:2605–20.
45. Shen H, Zhu H, Chen Y, Shen Z, Qiu W, Qian C, et al. ZEB1-induced LINC01559 expedites cell proliferation, migration and EMT process in gastric cancer through recruiting IGF2BP2 to stabilize ZEB1 expression. *Cell Death Dis*. 2021;12:349.
46. Zhou Y, Huang T, Siu HL, Wong CC, Dong Y, Wu F, et al. IGF2BP3 functions as a potential oncogene and is a crucial target of miR-34a in gastric carcinogenesis. *Mol Cancer*. 2017;16:77.

## ACKNOWLEDGEMENTS

This study was supported by Doctoral innovative talent base for new infections and immune regulation (RCJD2021B01), Laboratory Department of key medical specialty of Changning District Health Commission (20191001) and Local Innovative and Research Teams Project of Guangdong Pearl River Talents Program (2017BT01S131).

## AUTHOR CONTRIBUTIONS

WX and YL designed the experiments; WX and JW wrote the paper; YP, MT, YM and HS performed the experiments. All authors read and approved the final version of the paper.

## COMPETING INTERESTS

The authors declare no competing interests.

## ETHICS STATEMENT

All experimental procedures were approved by the Shanghai Tongren Hospital. This study was performed in accordance with the Declaration of Helsinki. Animal experiments were approved by the Animal Care Committee of Shanghai Tongren Hospital.

## ADDITIONAL INFORMATION

**Supplementary information** The online version contains supplementary material available at <https://doi.org/10.1038/s41419-022-05132-w>.

**Correspondence** and requests for materials should be addressed to Weihong Xu or Jiucun Wang.

**Reprints and permission information** is available at <http://www.nature.com/reprints>

**Publisher's note** Springer Nature remains neutral with regard to jurisdictional claims in published maps and institutional affiliations.



**Open Access** This article is licensed under a Creative Commons Attribution 4.0 International License, which permits use, sharing, adaptation, distribution and reproduction in any medium or format, as long as you give appropriate credit to the original author(s) and the source, provide a link to the Creative Commons license, and indicate if changes were made. The images or other third party material in this article are included in the article's Creative Commons license, unless indicated otherwise in a credit line to the material. If material is not included in the article's Creative Commons license and your intended use is not permitted by statutory regulation or exceeds the permitted use, you will need to obtain permission directly from the copyright holder. To view a copy of this license, visit <http://creativecommons.org/licenses/by/4.0/>.

© The Author(s) 2022